

# Radio Cosmology Lab | Exploring the Epoch of Reionization

Jacob Burba, Theodora Kunicki, Daniya Seitova,  
Samantha McGraw, Jasper Solt, Jonathan Pober  
Brown University Physics

# 21 cm @ COSMOLOGY



## Introduction

Following the recombination of hydrogen and release of the cosmic microwave background radiation, the baryonic matter of the universe consisted mostly of neutral hydrogen and helium. Gradually, small inhomogeneities collapsed and ignited into the first luminous structures. Energetic photons emitted from the first stars and quasars reionized the surrounding medium, producing ionized bubbles which grew and merged into the fully ionized intergalactic medium we see today. This *Epoch of Reionization* (EoR) remains a poorly-understood period of the universe's history which offers a wealth of cosmological and astrophysical information.

The Pober lab is part of an international effort to build instruments capable of studying the EoR. The neutral hydrogen (HI) of the EoR emits faintly at a wavelength of 21cm due to the hyperfine transition. This emission is unique to neutral hydrogen, and is anti-correlated with the ionized (HII) regions that fill the universe through the EoR. CMB constraints and quasar absorption spectra place the EoR within the redshift range  $6 < z < 12$ , which means 21cm emissions will reach us at meter scale wavelengths. This is accessible to modern radio interferometers, including the *Donald C. Backer Precision Array for Probing the Epoch of Reionization* (PAPER), the *Murchison Widefield Array* (MWA), and our newly observing *Hydrogen Epoch of Reionization Array* (HERA). Extracting this weak signal remains a challenge unprecedented in radio astronomy.

## Differential Brightness Temperature

$$\delta T_b = 27(1+\delta) x_{\text{HI}} \left(1 - \frac{T_{\text{CMB}}}{T_{\text{spin}}}\right) \left(\frac{\Omega_b h^2}{0.0223}\right) \left(\frac{1+z}{10} \frac{0.15}{\Omega_m h^2}\right)^{1/2} \left[\frac{H(z)/(1+z)}{\partial_r v_r}\right] \text{ mK}$$

Annotations: Density perturbation, Neutral fraction, Spin excitation, Baryon and matter mass fractions, Peculiar velocities

The differential brightness temperature  $\delta T_b$  is the contrast between the intensity of 21 cm emissions/absorptions against the Cosmic Microwave Background. Its full expression is related to cosmological (green) and astrophysical (red) parameters. Figure 1 shows the evolution of the spherically-averaged *global* 21 cm brightness temperature.

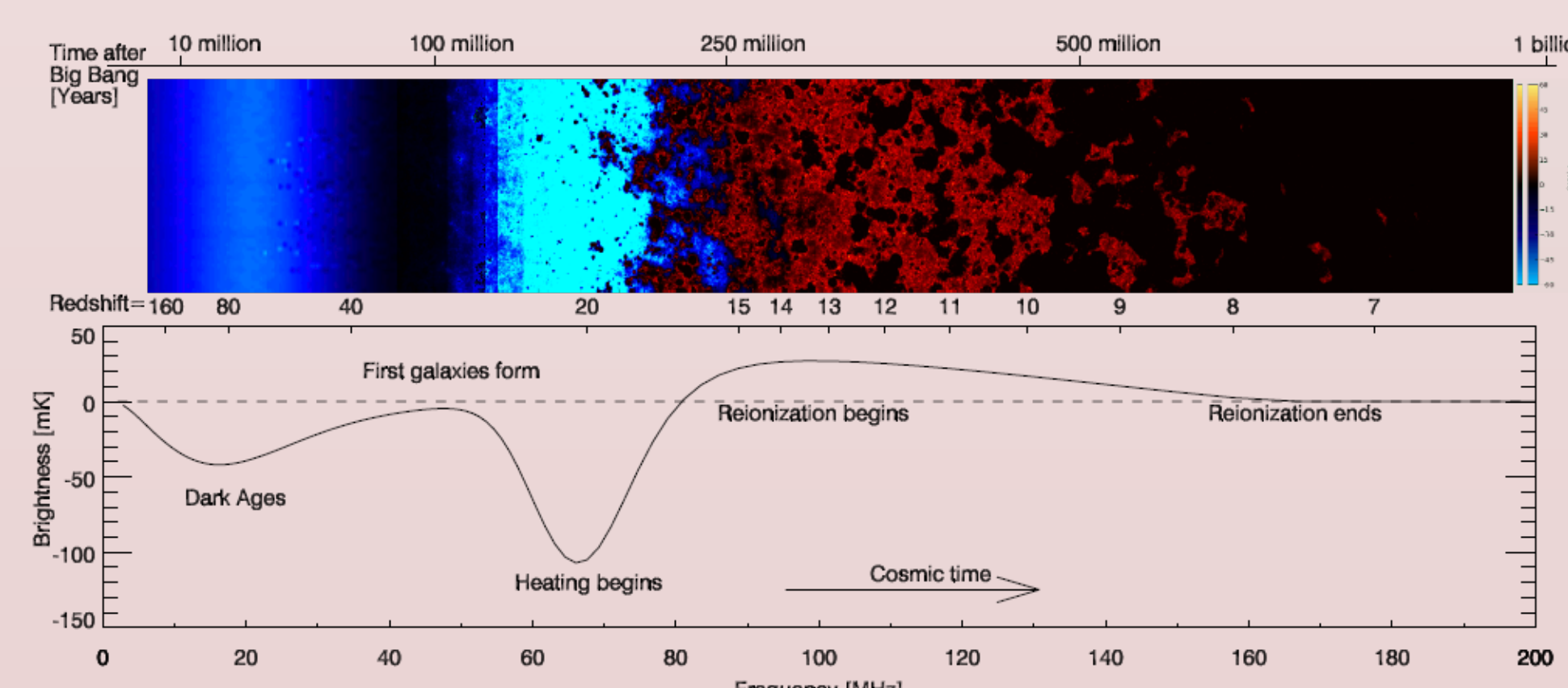


Figure 1: The global differential brightness temperature,  $\delta T_b$ , evolution over redshift  $6 < z < 160$ .  $\delta T_b$  becomes observable when the spin temperature  $T_s$  decouples from the CMB temperature,  $T_{\text{CMB}}$ . Source: Pritchard & Loeb. Nature 468.7325 (2010): 772-773.

The major challenge of EoR detection is the overwhelmingly bright foreground contamination. The expected EoR signal is  $\sim 5$  orders of magnitude weaker than known foreground sources, such as diffuse emission from the Galaxy and extragalactic point sources. Removing these foregrounds, as well as instrumental noise, is a nontrivial problem. In addition to galactic and extragalactic foregrounds we must also contend with Radio Frequency Interference (RFI).

## Bayesian Data Analysis

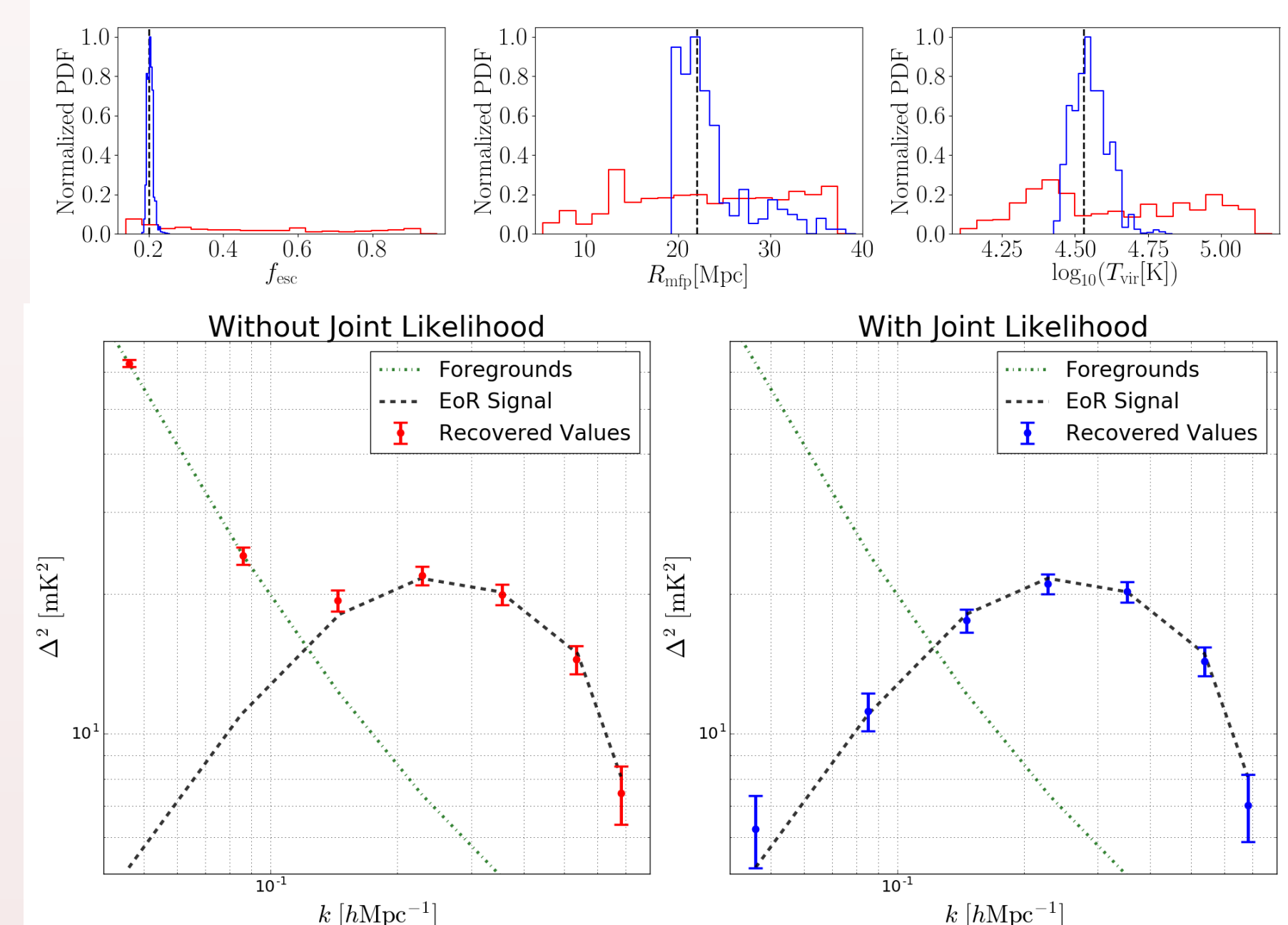


Figure 2: [Top] Constraints on the escape fraction of ionizing radiation from galaxies,  $f_{\text{esc}}$ , the mean free path of ionizing photons through the intergalactic medium,  $R_{\text{mfp}}$ , and the minimum virial temperature of halos hosting galaxies,  $T_{\text{vir}}$  derived from power spectrum estimates accessible using the existing HERA analysis pipeline (red) and Bayesian forward modeling analysis of simulated HERA data (blue). [Bottom] Recovered EoR power spectrum from simulated HERA data using a Bayesian power spectral estimation methodology with i) polynomial foreground parametrization (red points, left) and ii) an optimized power law parametrization derived using Bayesian model selection (blue points, right).

A statistically robust analysis of the data is essential to avoid a spurious or mischaracterised detection of the EoR signal. We have developed an advanced Bayesian mathematical data analysis framework designed to meet this need. By extending the range of spatial scales on which the EoR signal can be reliably measured, this framework brings forward a first detection of the EoR signal and facilitates further analysis of the data to probe the state of dark matter in the early Universe.

## Machine Learning Reionization

Our goal is to use Machine Learning to extract the temporal evolution of reionization (characterized by the mean, midpoint, and duration) from simulations that account for the degrading effects of the radio telescope. To extract the physical parameters of reionization, a Convolutional Neural Network (CNN) was trained with simulated data. The resulting model was able to extract the mean and midpoint to within  $\pm 1\%$  and the duration to within  $\pm 10\%$  of their true values.

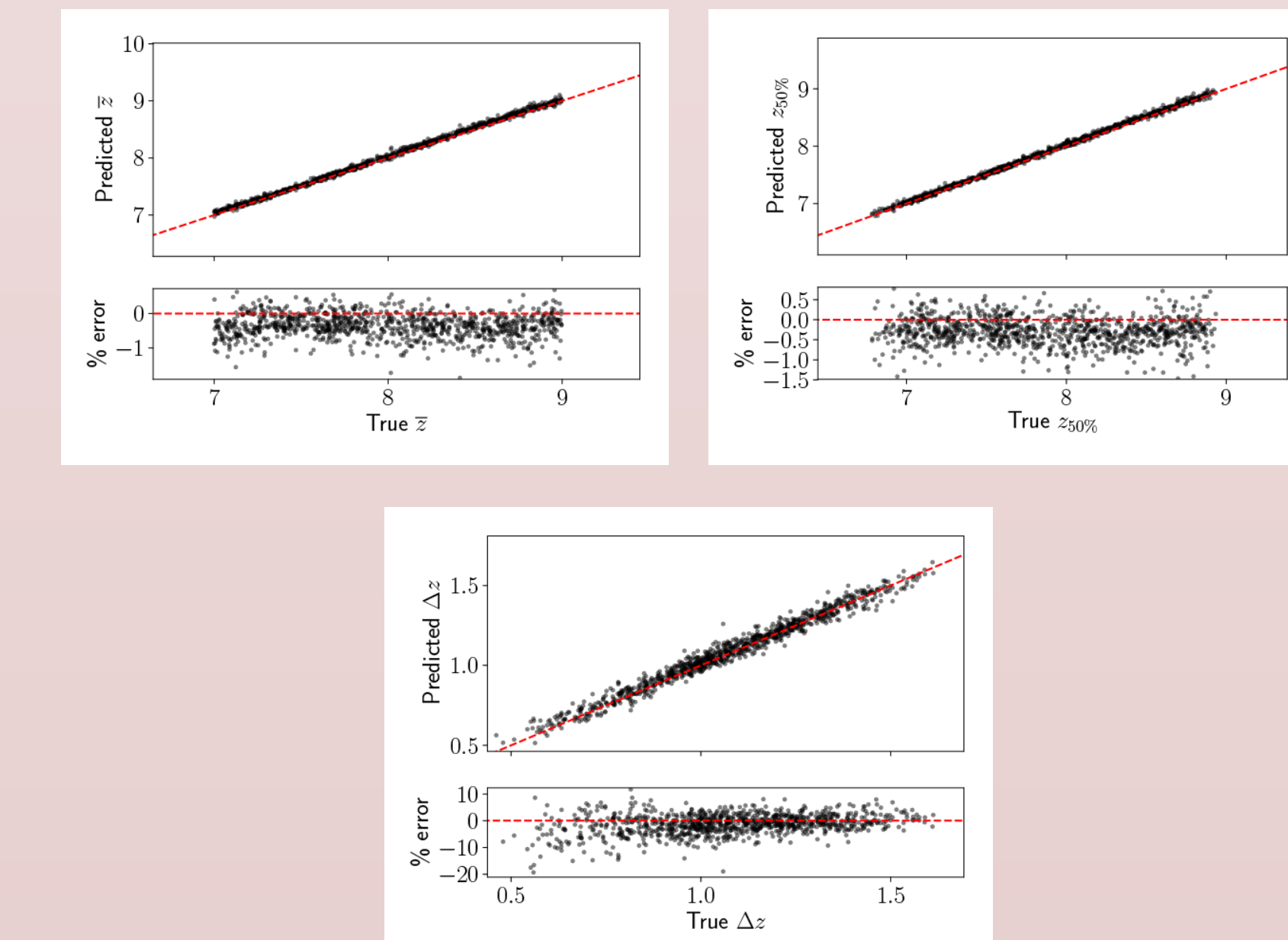


Figure 3: Convolutional Neural Network predictions of the mean (top left), midpoint (top right), and duration (bottom) of semi-numerical simulations of reionization. Higher error in the duration may be a result of the redshift intervals of the training data approaching the duration of reionization.

## Simulation

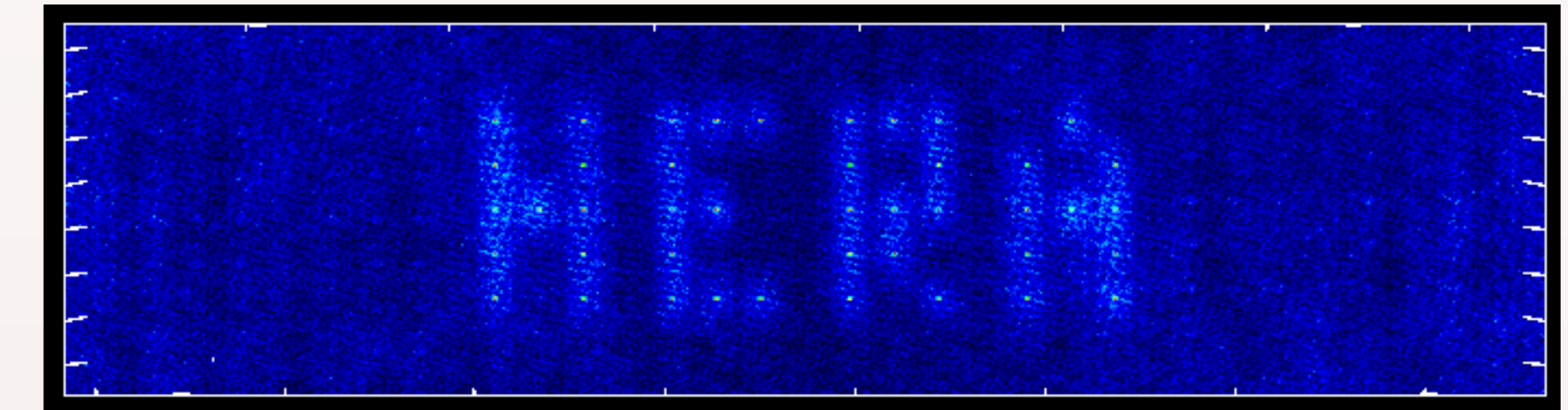


Figure 4: An image produced from simulated data from *pyuvsim*, of a mock catalog that spells out "HERA" in point sources at the zenith.

Radio interferometers have complicated responses which can easily introduce systematics that overwhelm the desired signal. End to end simulation is used to check for these effects and find ways to mitigate them. These simulations start with a known sky model, calculate visibilities via the interferometer measurement equation (1), pass these through an analysis pipeline, and compute power spectra and other data products. Often this process reveals effects that had not yet been seen in data, but are later observed.

$$V_{ij} = \int d\Omega \mathcal{J}_i \mathcal{C} \mathcal{J}_j^\dagger \exp(-2\pi i \vec{v} \cdot \vec{b}_{ij} \cdot \hat{s}/c) = \begin{pmatrix} V_{ij}^{pp} & V_{ij}^{pq} \\ V_{ij}^{qp} & V_{ij}^{qq} \end{pmatrix} \quad (1)$$

Eqn. (1) gives the visibilities for all pairs of antenna feeds, given the antenna Jones matrices  $\mathcal{J}$  and sky coherency matrix  $\mathcal{C}$ . Evaluating this for large sky models and antenna arrays requires great computational resources, so simulators often make simplifying assumptions that cut runtime at the expense of accuracy.

*pyuvsim* is a new instrument simulator, developed with an *accuracy first, efficiency second* philosophy that ensures that we take into account all factors known to impact an interferometer signal. These factors include the full polarized response, precise source positioning, empirical primary beams, and full horizon to horizon sky coverage. It has served as a verification tool for other simulators, and will continue to see performance improvements in the coming years.

## Calibration

Interferometric arrays seeking to measure the 21 cm signal from the EoR must contend with overwhelmingly bright emission from foreground sources. Accurate recovery of the 21 cm signal will require precise calibration of the array, and several new avenues for calibration have been pursued in recent years. Current calibration efforts for EoR observations largely fall into two camps: sky-based calibration using deep foreground catalogs and forward modeling of the instrument visibilities, and redundant calibration that foregoes a sky model but requires the antennas be placed on a regular grid. A further exploration of combining both approaches has been pushing on to mitigate the contamination in the power spectrum.

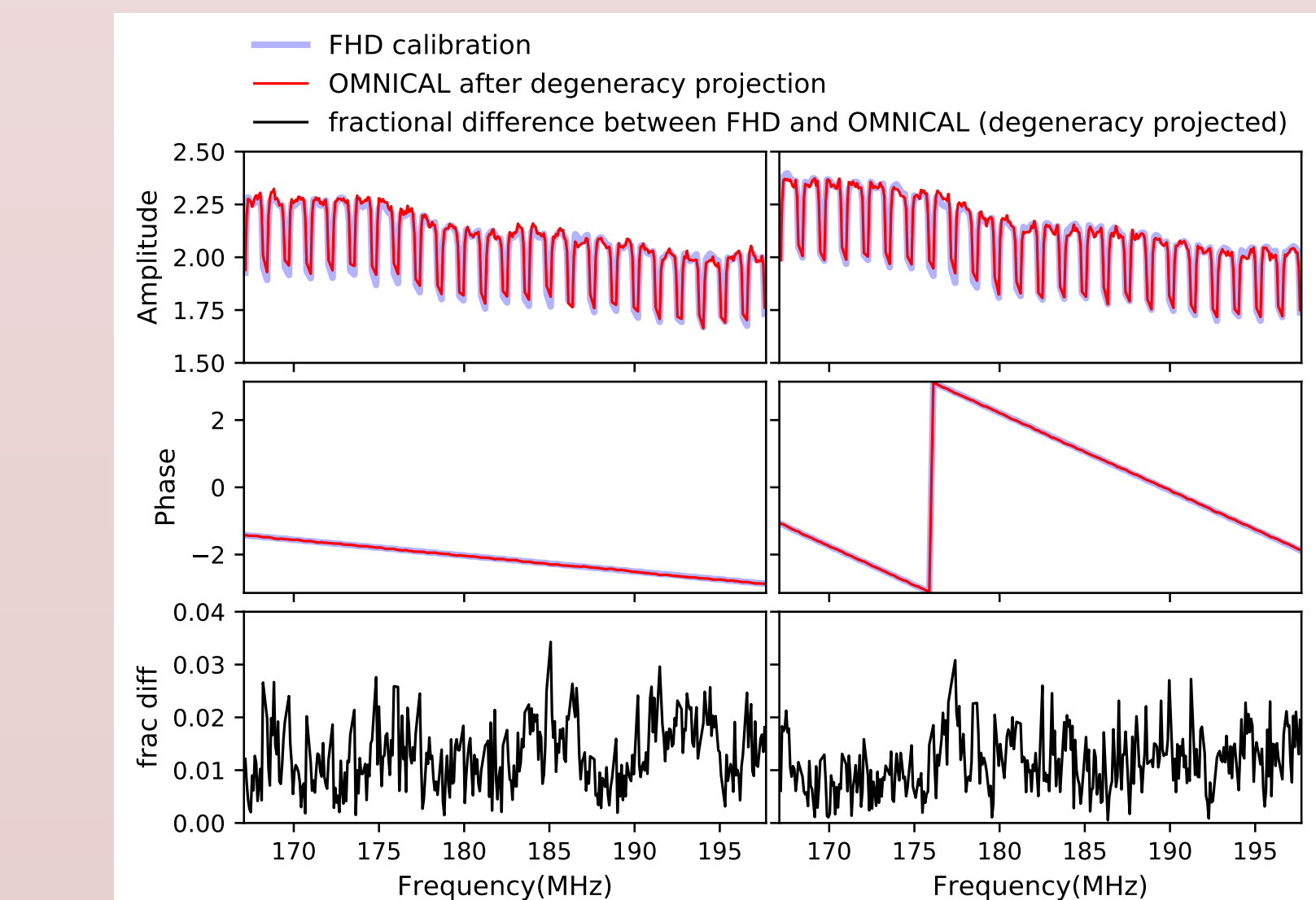


Figure 5: 30 minutes averaged gain calibrations of 2 MWA PhaseII tiles. Upper: Gain amplitude; Middle: Gain phase. Lower: fractional difference between sky based (FHD) and redundancy based (OMNICAL) solutions with degeneracy projected. Blue: FHD solutions; Red: OMNICAL solutions after projecting degeneracy.

## Observatories

The Epoch of Reionization signal is expected within the 50 to 200 MHz frequency range, which overlaps with FM radio broadcast bands and numerous other RFI sources. This interference can be reduced by choosing remote locations for building observatories.

### Murchison Widefield Array (MWA)

The MWA is one of the three Square Kilometer Array (SKA) Precursor telescopes located at the Murchison Radio-astronomy Observatory (MRO) in Western Australia. It is a low frequency telescope operating at 80-300MHz, with a processed bandwidth of 30.72 MHz. The Phase I of MWA consists of 128 tiles pseudo-randomly distributed over 3 km diameter area. The newly upgraded Phase II MWA has an additional 128 tiles, with 72 of them arranged as two hexagonal cores.



Figure 6: MWA - Located in the Murchison Radio-astronomy Observatory in Western Australia.

### Hydrogen Epoch of Reionization Array (HERA)

The Hydrogen Epoch of Reionization Array is a 2<sup>nd</sup> generation radio interferometer currently under construction in the Karoo desert of South Africa. When completed, HERA will comprise 350 14.6 m zenith-pointing dishes, with a 320-dish close-packed hexagonal core and 30 "outrigger" dishes. Each dish will carry dual polarization antenna feeds, sensitive to a bandpass of 50 to 250 MHz ( $z \sim 5.68 - 28.4$ ).



Figure 7: (Top) HERA - Located in the Karoo desert in South Africa. (Bottom) Jacob, Daniya, and Theo wiring up a HERA node on site.